



University
of Glasgow

Xu, J., Hou, L., Deng, Q., Han, L., Liang, S., Zhu, H., and Marsh, J. (2016)
Optoelectronic THz Frequency Synthesizer Based on a Multiple Laser Photonic
Integrated Circuit. In: CLEO: Science and Innovations, San Jose, California, USA,
5-10 June 2016, STh11.1. ISBN 9781943580118

There may be differences between this version and the published version. You are
advised to consult the publisher's version if you wish to cite from it.

<http://eprints.gla.ac.uk/120183/>

Deposited on: 14 June 2016

Enlighten – Research publications by members of the University of Glasgow
<http://eprints.gla.ac.uk>

Optoelectronic THz Frequency Synthesizer Based on a Multiple Laser Photonic Integrated Circuit

Junjie Xu¹, Lianping Hou^{*2}, Qiufang Deng¹, Liangshun Han¹, Song Liang¹, Hongliang Zhu¹, John H. Marsh²

¹Institute of Semiconductors, No. A35, East Qinghua Road, Haidian District, Beijing 1000083, P.R. China

²School of Engineering, University of Glasgow, Glasgow, G12 8LT, U.K.

*Corresponding author: lianping.hou@glasgow.ac.uk

Abstract: An optoelectronic synthesizer based on photonic integrated circuits is reported for use in THz communication systems. The source has widely selectable channels, a broad range of continuous tuning (0.254-2.723 THz), and excellent resilience against failure.

OCIS codes: (140.3490) Distributed-feedback lasers; (230.3120) Integrated optics device; (300.6495) Spectroscopy, terahertz.

Wireless data traffic has increased dramatically during recent years. In addition to the traditional wireless spectrum bands, in future the THz frequency band between 0.1 and 10 THz will be needed to support extremely high data rates [1] and alleviate the spectral scarcity and capacity limitations of current wireless systems [2]. Terahertz sources based on semiconductor devices have the advantage of a small form factor and similar packaging to traditional components, enabling their use in applications such as ultra-high speed on-chip communications, data storage [3], data center communications, and satellite to satellite communications [4]. Recently, a monolithic THz source has been reported using a quantum cascade laser [5], with the ability to tune over the range 1-5 THz at room temperature. Dual cascaded DFBs integrated with a phase section have also been designed to generate THz waves [6, 7], with a continuous tuning range from 0.3 THz to >1.34 THz [7]. Although these devices cover a wide THz tuning range, additional components, including modulators to encode data, will be needed in real communications applications, which will considerably increase their cost and complexity. The use of an optical carrier offers considerable advantages for manipulating and encoding THz signals prior to conversion to THz radiation in a detector/antenna. Here we report the use a photonic integrated circuit (PIC) as a THz synthesizer which also has the ability to encode data. Previous rare studies on PIC transmitters for wireless communications were limited to the gigahertz frequency range, such as the report by Gael Kervella from the III-V Lab of Alcatel Lucent which explored the range 30 to 200 GHz [8].

In this paper, we present a monolithically-integrated, InP-based PIC designed to generate THz signals on an optical carrier by difference-frequency generation (DFG) through mode-beating light from pairs of DFB lasers. In order to ensure a narrow THz linewidth, the cavity length of each laser was made relatively long at 1.155 mm, and the light was modulated using individual electro-absorption modulators (EAMs) external to the lasers. The EAMs could be used to match the signal levels from the lasers and to encode data. The lasers were tuned by changing their drive currents, so frequencies from 0.254 to 2.723 THz could be selected continuously by biasing particular pairs of DFBs at appropriate currents. Certain THz frequencies could be generated from more than one laser pair; this redundancy can be important in applications where reliability is extremely critical such as satellite to satellite communications. The PIC contained 4 lasers, so up to three different THz channels could be generated and modulated simultaneously, multiplying the potential data throughput by the same factor.

The epitaxial structure and fabrication processes are similar to those described in [9]. An optical micrograph and the dimensions of the device are shown in Fig. 1(a). The grating periods (Λ) are 243, 244, 245, 246 nm from CH1 to CH4 respectively. The gratings are of first-order with a 50% duty cycle and formed by etching recesses of depth $d = 0.6 \mu\text{m}$ into the sidewalls of the waveguide, as shown in Fig. 1(b). A $\lambda/4$ phase shift is inserted in the center of the cavity of each DFB laser (Fig. 2(b)) to ensure single longitudinal mode (SLM) operation. The EAMs have a length of $150 \mu\text{m}$, capable of digital modulation at $>5 \text{ GHz}$ with a clear open eye pattern [10].

The chip was mounted on a temperature controlled copper sink and all tests were taken with the temperature set at $20 \text{ }^\circ\text{C}$. Fig. 2(a) presents the spectrum with all four DFBs driven simultaneously. The measured linewidths of the four DFB laser are all around 3 MHz at a bias current of 100 mA. DFB1 was selected as the base laser with its external EAM floating, while the others were selected as lasers which could be modulated via each of the EAMs. Up to three THz communication channels can therefore be established. All of the four DFBs in the array can be tuned by varying their drive current. Each DFB has a wavelength tuning range of $\sim 4 \text{ nm}$, so the wavelength difference between DFB1 and DFB4 can be as large as 21.61 nm. No mode hopping was observed during current tuning. The THz frequencies are created by DFG between beams from pairs of DFB lasers. Despite the tuning ranges of these four DFBs being separated by several nanometers, the difference frequency can be tuned continuously, as is depicted in Fig. 2(b). The colored areas represent all the possible frequencies that can be realized by biasing the corresponding DFB currents. From the dashed lines in Fig. 2(b), we can separate the continuous THz tuning range

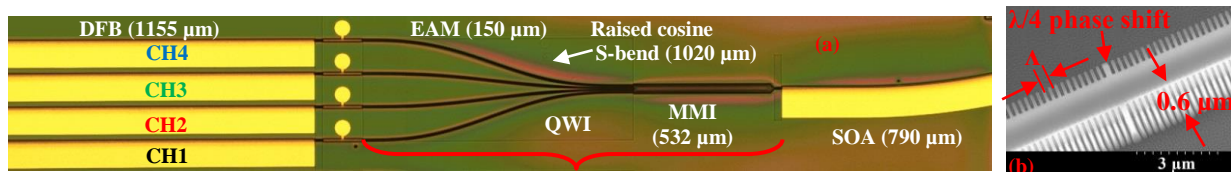


Fig. 1. (a) Optical micrograph of the overall laser array, (b) SEM showing first order side-wall gratings with 0.6 μm recess depth.

into five channel regions (CRs) for discussion, which have different redundancies. CR1 (top, blue) in the graph results from DFG between light from DFB1 and DFB4. As can be seen, there is no redundancy in this region, but for CR2 to CR5 there are always at least two combinations of diodes that be used. In CR2, for example, the frequency band from 1.717 THz to 1.933 THz exhibits 3-fold redundancy between the blue, pink and green regions, which arise from $\Delta\lambda_{DFB4-DFB1}$, $\Delta\lambda_{DFB3-DFB1}$ and $\Delta\lambda_{DFB4-DFB2}$, respectively. If DFB1 were to fail, this THz channel could be generated by using the corresponding frequencies from $\Delta\lambda_{DFB4-DFB2}$, or, if DFB2 were to fail, this THz channel could be generated using $\Delta\lambda_{DFB4-DFB1}$ or $\Delta\lambda_{DFB3-DFB1}$. In other words, one alternative combination choice exists if DFB1 fails, and two alternatives if DFB2 fails. Furthermore, if DFB1 and DFB3 both fail, these THz channels could be maintained by using DFG from $\Delta\lambda_{DFB4-DFB2}$.

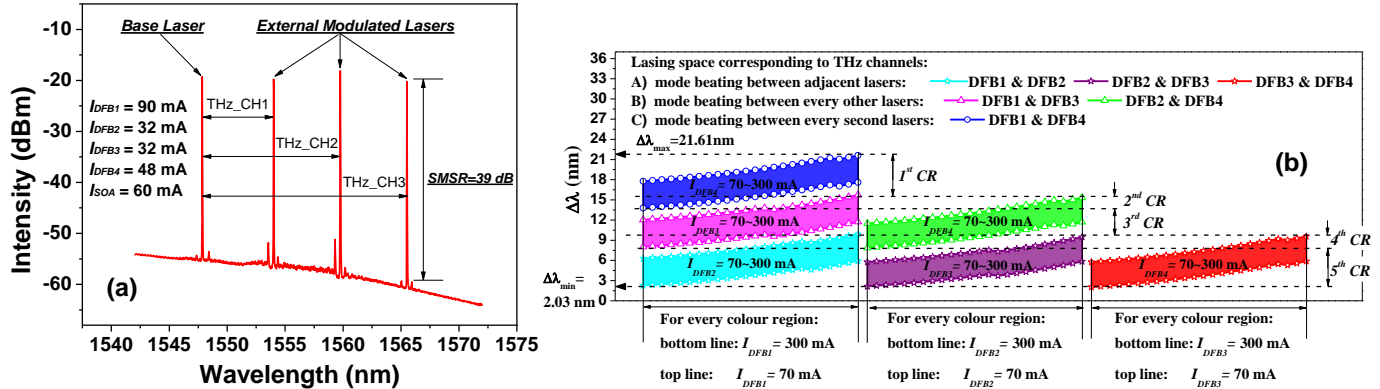


Fig. 2. (a) The measured spectrum with all four channels operating simultaneously with $I_{DFB1} = 90$ mA, $I_{DFB2} = 32$ mA, $I_{DFB3} = 32$ mA, $I_{DFB4} = 48$ mA and $I_{SOA} = 60$ mA and EAMs floating. (b) The wavelength difference between every combination of pairs of DFBs.

Fig. 3(b) shows the mode-beating signals measured using an optical autocorrelator. The five normalized second-harmonic generation (SHG) curves correspond to the optical spectra in the same colors in Fig. 3(a), and these curves represent typical results for the five THz channel regions presented in Fig. 2(b). The clear DFG signal from two narrow linewidth DFBs results in a flat, sinusoidal SHG trace. The frequencies correspond to various THz channels which can be used as carrier frequencies for THz wireless communications.

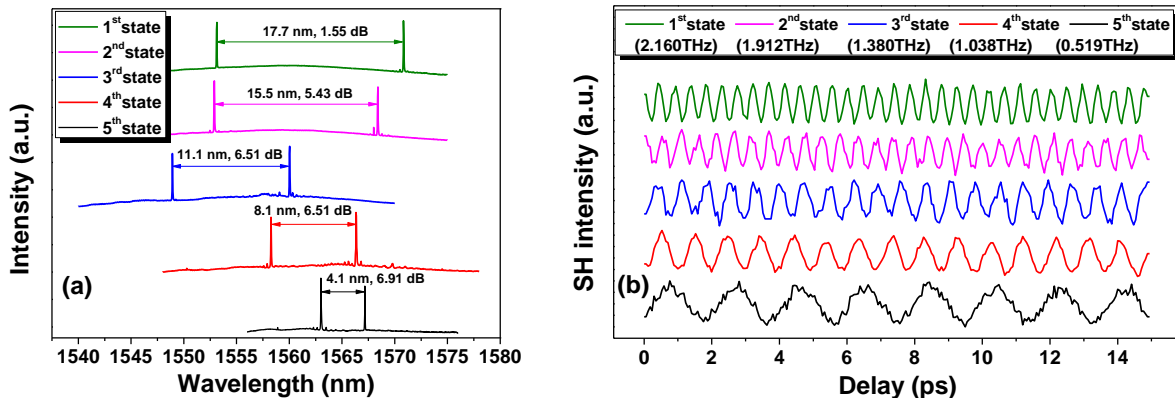


Fig. 3. (a) Typical spectra for five frequency ranges of the PIC; the differences of peak wavelength and intensity between the peaks are shown. (b) Normalized second-harmonic generation (SHG) correlation traces measured simultaneously with the spectra shown in (a).

In summary, PIC-based optoelectronic synthesizer for THz communication systems has been demonstrated for the first time. The PICs were fabricated using simple side-wall gratings and QWI technologies, which eliminate the multiple stages of crystal re-growth required in traditional approaches and so reduce cost. The PIC produces up to three mode-beat THz optical signals simultaneously and can be tuned over the range 0.254 to 2.723 THz with no gaps. The wide tuning range opens up applications such as THz wireless communications between CPUs, and the high level of redundancy makes the source particularly suitable where rigorous reliability is required, such as inter-satellite communications. Along with developments in THz antennas, this PIC-based synthesizer will be a significant enabler of THz wireless systems in the near future.

This work has been sponsored by the National Natural Science Foundation of China under grant no.61320106013 through a major international joint research program with UK.

References

- [1] T. Kürner et al., J Infrared Milli Terahz Waves. **35**, 53-62(2014).
- [2] S. Koenig et al., Nature Photon. **7**, 977-981 (2013).
- [3] I. F. Akyildiz et al., Physical Communication. **12**, 16-32 (2014).
- [4] M. J. Fitch et al., Johns Hopkins APL Tech. Dig. **25**, 348-355 (2004).
- [5] S. Jung et al., Nat. Commun. **5**, 4267 (2014).
- [6] N. Kim et al., Opt. Express. **17**, 13851 (2009).
- [7] K. H. Park et al., Proc. of SPIE. 8261, 826103 (2012).
- [8] G. Kervella, et al., Photon. Res. **2**, B70-79 (2014).
- [9] L. Hou et al., Photon. Technol. Lett. **23**, 1064-1066 (2011).
- [10] L. Hou et al., IEEE Photon. Technol. Lett. **25**, 1169-1172 (2013).